



Faculty of Science - University of Benghazi

Libyan Journal of Science & Technology

journal home page: www.sc.uob.edu.ly/pages/page/77

Numerical solution of Poisson's equation in two-dimensions (2D) for linearly-graded p-n junction of silicon

Ali Y. Darkwi*, Fathi Y. Elfituri

Department of Physics, Faculty of Science, University of Benghazi

Highlights

- **Linear grading of charge impurities in the depletion layer was implemented. First, the calculation was carried out for one-dimension (1D), then extended into two-dimensions (2D)**
- **Close to the metallurgical junction of p-n, the charge density follows linearity on both sides, however, far away of the junction it deviated from linearity, due to the exponential form of free charge density.**
- **The electric field and electrostatic potential distributions within the depletion layer are significantly affected by free carriers.**

ARTICLE INFO

Article history:

Received 17 June 2020

Revised 19 March 2021

Accepted 25 March 2021

Keywords:

Charge density, impurity, depletion layer, finite difference method.

*Address of correspondence:

E-mail address: alidarkwi@uob.edu.ly

A. Y. Darkwi

ABSTRACT

In this paper, the numerical solution of Poisson's equation in two-dimension (2D) of p-n junction of silicon has been carried out using Neumann and Dirichlet boundary conditions. Assumption of linearly grading impurities doping has been used for analysis of charge density. The calculation has been done for different dopant concentration rates of impurities. The aim of this calculation is to find out the profile of the potential and electric field within depletion layer.

1. Introduction

The p-n junction is a fundamental building block of semiconductor devices. One side of a semiconductor is doped with an acceptor impurity and another side with a donor impurity. The impurity distribution in p-n junction can be presented with the simplified models called abrupt junction and the linearly graded junction (Henry *et al.*, 1982; Zambuto 1989). In a linearly graded junction, the doping concentration varies almost linearly with the distance from the junction.

In the theory of p-n junction in semiconductor, Shockley presented the first analysis applicable to structure containing a linearly-graded impurity atom distribution in the depletion layer (Shockley, 1949). With the charge density of impurities and mobile charges, Poisson's equation can be solved to obtain the potential and electric field within the depletion layer. Although this equation does not appear to have an analytical solution, many articles (Green 1982; Neamen 1997; Zambuto 1989) deal with an analytical treatment in order to simplify the analysis. The exponential variation of mobile charges with the potential in the space-charge region leads to the solution of Poisson's equation to be non-linear. Hence, various methods such as the relaxation method, an iterative algorithm are essential for the numerical solution of such problems (Fathi and Darkwi 2006; Alexei and Sajejev 2012).

It often happens that, the equation to be solved may contain more than one variable, x, y, z . In this paper, the solution is devoted

to solving Poisson's equation in two dimensions (2D) within a rectangle with Neumann and Dirichlet boundary values. We derived the solution for the case of p-n junction at equilibrium (zero bias). Numerous papers have been devoted to numerical solution of Poisson's equation (Achoyan *et al.*, 2002; Kosec and Trobec 2015). Some work has been done (Akinpelu *et al.*, 2018) on numerical simulation of Poisson's equation in 2D for an abrupt and linearly graded charge densities distribution in the depletion layer. However, they did not show explicitly the profile of the electric field within the depletion layer.

In this paper, we present a numerical method for the solution of Poisson's equation using the successive over-relaxation (SOR) technique. The method is based on transforming Poisson's equation into a system of nonlinear algebraic equations. Linear grading of charge impurities in the depletion layer was implemented. First, the calculation was carried out for one-dimension (1D), and then extended into two-dimensions (2D).

2. Theory

The schematic diagram of the p-n junction diode is shown in Fig. 1. When the metallurgical junction is preform between two types of semiconductors, electrons move to p-type and holes move to n-type until fermi levels become coincide on both sides in equilibrium. Hence, near the junction, fixed positive charges are left in n-type while negative charges in p-type creating an internal electric field and a built-in potential that prevent the moving of more charges across the junction. The space charge region or depletion

layer exists on either side of the metallurgical junction that separates the n-and p-type regions. To do quantitative analysis of physical parameters, the distribution of charges within the depletion layer may be represented by geometrical functions such as abrupt or linear grading junction (Sze 1981; Zambuto 1989).

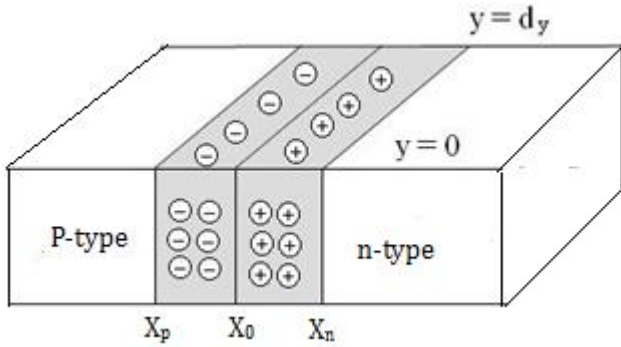


Fig. 1. The p-n junction

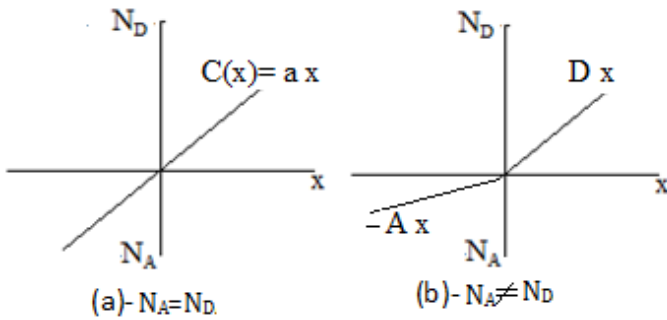


Fig. 2. Linearly grading distribution of impurity charges: (a)- equal dopant $N_A=N_D$, and (b)- non-equal dopant $N_A \neq N_D$.

In the space charge region, the relationships among the charges and potential are represented by Poisson’s equation on 2-D case as:

$$\frac{d^2\phi(x,y)}{dx^2} + \frac{d^2\phi(x,y)}{dy^2} = -\frac{q}{\epsilon} (N_D - N_A + p(x) - n(x)) \quad (1)$$

Where $\phi(x,y)$ is the potential, ϵ is the dielectric of the media, q is the electric charge, N_D donor, and N_A acceptor densities. The $n(x)$ and $p(x)$ are the electron and hole density respectively, which are given by

$$p(x) = n_i e^{-\frac{q\phi(x,y)}{KT}} \quad (2)$$

and

$$n(x) = n_i e^{\frac{q\phi(x,y)}{KT}} \quad (3)$$

where n_i is the intrinsic concentration of charges, K is Boltzmann’s constant, and T is temperature. Because of the exponential terms in the expression for charge density on the potential $\phi(x,y)$, the analytical solution of Poisson’s equation becomes difficult, hence, a numerical solution is essential for this case.

Using the finite difference method to L-side of the Eq. (1), yielding (Benyam, 2015):

$$\frac{\phi_{i+1,j} - 2\phi_{i,j} + \phi_{i-1,j}}{h_x^2} + \frac{\phi_{i,j+1} - 2\phi_{i,j} + \phi_{i,j-1}}{h_y^2} = f(x_{i,j}, y_{i,j}, \phi_{i,j}) \quad (4)$$

Where h_x and h_y are the distance between two successive grid points along x, y respectively. For linear impurity doping, the function $f(x_{i,j}, y_{i,j}, \phi_{i,j})$ is given by

$$f(x_{i,j}, y_{i,j}, \phi_{i,j}) = -\frac{q}{\epsilon} \left(a x_{i,j} - 2n_i \sinh\left(\frac{q\phi_{i,j}}{KT}\right) \right) \quad (5)$$

Rearranging Eq. (4) and for $h_x = h_y = h$ one can find

$$\phi_{i,j} = \frac{\phi_{i+1,j} + \phi_{i-1,j} + \phi_{i,j+1} + \phi_{i,j-1} - h^2 f(x_{i,j}, y_{i,j}, \phi_{i,j})}{4} \quad (6)$$

For $h_x \neq h_y$, Eq. (6) reduce to

$$\phi_{i,j} = \frac{h_y^2(\phi_{i+1,j} + \phi_{i-1,j}) + h_x^2(\phi_{i,j+1} + \phi_{i,j-1}) - h_x^2 h_y^2 f(x_{i,j}, y_{i,j}, \phi_{i,j})}{2(h_x^2 + h_y^2)} \quad (7)$$

Implementing the boundary condition, one can find the potential at each inner grid point using the iteration method.

a-The Neumann boundary condition

The potential at edges of depletion layer (x_n) and ($-x_p$) is given by (Zambuto, 1989)

$$\phi_n = \frac{qN_D}{2\epsilon} x_n^2 \quad (8)$$

$$\phi_p = -\frac{qN_A}{2\epsilon} x_p^2 \quad (9)$$

The grading point potential $\phi_{(i,j)}$ along $x = x_n$ and $0 \leq y \leq d_y$ will be:

$$\phi_{(N+1,j)} = \phi_n \quad \text{for } 0 \leq j \leq M+1 \quad (10)$$

Similarly, along $x = -x_p$ and $0 \leq y \leq d_y$ will be:

$$\phi_{(0,j)} = \phi_p \quad \text{for } 0 \leq j \leq M+1 \quad (11)$$

The N and M are the number of the grid points along x and y respectively, see Fig. 3.

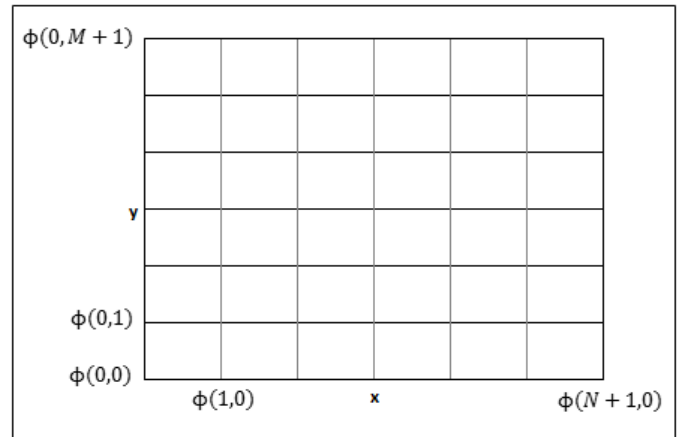


Fig. 3. Gridding points in two dimensions

b-The Dirichlet boundary condition

Fig. 1 shows the electric field due to the distribution of charges is directed along the x -axis. Consequently, there is no field along the y -axis, hence $E = -d\phi/dy = 0$. At $y = 0$ we get

$$E_y = -\frac{(\phi_{(i,j+1)} - \phi_{(i,j-1)})}{h_y} = 0 \quad (12)$$

Or

$$\phi_{(i,j-1)} = \phi_{(i,j+1)} \quad (13)$$

Substituting Eq. (13) in Eq. (7), we get the potential at edge $y=0$ and x follow the indices i where $0 \leq i \leq N$ as,

$$\phi_{i,0} = \frac{h_y^2(\phi_{i+1,0} + \phi_{i-1,0}) + 2h_x^2\phi_{i,0} - h_x^2 h_y^2 f(x_{i,0}, y_{i,0}, \phi_{i,0})}{2(h_x^2 + h_y^2)} \quad (14)$$

Similarly, at edge $y = d_y$, we get;

$$\phi_{i,M+1} = \frac{h_y^2(\phi_{i+1,M+1} + \phi_{i-1,M+1}) + 2h_x^2\phi_{i,M+1} - h_x^2 h_y^2 f(x_{i,M+1}, y_{i,M+1}, \phi_{i,M+1})}{2(h_x^2 + h_y^2)} \quad (15)$$

The boundary conditions Eq. (10), Eq. (11), Eq. (14), and Eq. (15), with the initial gauss of inner grade points of $\phi_{i,j}$, Eq. (7) can be solved by using the successive over-relaxation (SOR) method.

3. The depletion layer approximation

The width of depletion rejoin in a p-n junction can be estimated by depletion layer approximation. This assuming that the carrier concentration ($n(x)$ and $p(x)$) is negligible compared to the net doping concentration (N_A and N_D) in the region straddling the metallurgical junction. For a linearly graded junction of Fig. 2a the impurity concentration is given by (Zambuto 1989; Kennedy and O'Brien 1967)

$$N_D - N_A = a x \quad -x_p \leq x \leq x_n \quad (16)$$

where a is constant called dopant rate with units cm^{-4} .

Consequently, with the above assumption Poisson's equation can simply be integrated yielding built-in potential ϕ_{bi} related to the depletion layer.

$$\phi_{bi} = \frac{q a x_d^3}{12 \epsilon} \quad (17)$$

where x_d is total depletion layer, for $N_D = N_A$, one can find $x_d = 2 x_n$. Then, the proportionality constant a is given by

$$a = \frac{N_D}{x_n} = \frac{2 N_D}{x_d} \quad (18)$$

The built-in potential can also be computed from the equation:

$$\phi_{bi} = \frac{kT}{q} \ln \left(\frac{N_D N_A}{n_i^2} \right) \quad (19)$$

Using Eq. (17) and Eq. (18), one can find the depletion layer by

$$x_d = \sqrt{\frac{6 \epsilon \phi_{bi}}{q N_D}} \quad (20)$$

For linearly graded junction of Fig. 2b, where A and D are rates of variation of acceptor and donor respectively, given by

$$A = \frac{N_A}{x_p} \quad (21)$$

and

$$D = \frac{N_D}{x_n} \quad (22)$$

In this case, the depletion region charge neutrality condition becomes

$$A x_p^2 = D x_n^2 \quad (23)$$

Integrating Poisson equation and using boundary condition, yielding approximate depletion layer in each side of the junction as (Zambuto, 1989)

$$x_p = \sqrt[3]{\frac{3 \epsilon}{q A} \frac{\sqrt{D}}{\sqrt{A} + \sqrt{D}}} \phi_{bi} \quad (24)$$

$$x_n = \sqrt[3]{\frac{3 \epsilon}{q D} \frac{\sqrt{A}}{\sqrt{A} + \sqrt{D}}} \phi_{bi} \quad (25)$$

And quasi-Fermi levels

$$\phi_p = -\frac{q A}{3 \epsilon} x_p^3 \quad (26)$$

$$\phi_n = \frac{q D}{3 \epsilon} x_n^3 = \frac{q A}{3 \epsilon} x_p^3 \sqrt{\frac{A}{D}} \quad (27)$$

4. Result and Discussion

A silicon p-n linear-graded junction with $N_D=10^{14} \text{ cm}^{-3}$ and $N_A=10^{14} \text{ cm}^{-3}$ has been implemented in the calculation. Finite difference method by implying successive over-relaxation (SOR), a solution of Poisson's equation in two-dimension has been obtained using Newman and Dirichlet boundary condition. In the case of considering only fixed charge density due to impurity within the depletion layer, Poisson's equation was solved analytically. Fig. 4 shows the linearly fixed charge distribution of ionized impurities within the depletion layer. Fig. 5 and Fig. 6 show the profile of potential and electric field within the depletion layer due to charge distribution. The numerical result obtained was in quite well agreement with the analytical.

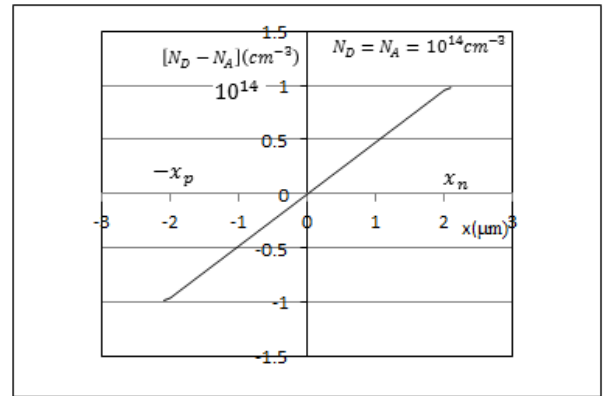


Fig. 4. The linearly fixed charge density of impurities [N_A , N_D] within the depletion layer

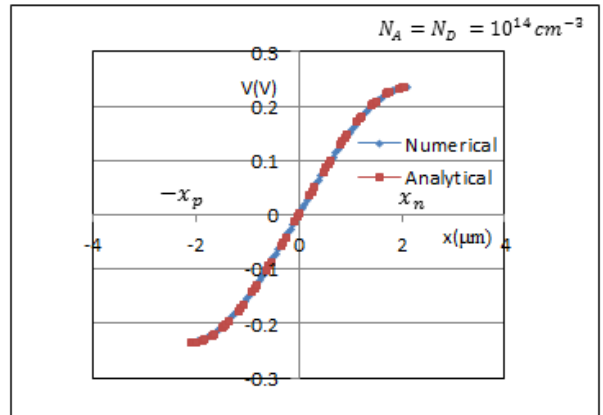


Fig. 5. Electrostatic potential for fixed charge density of impurities [N_A , N_D] within depletion layer

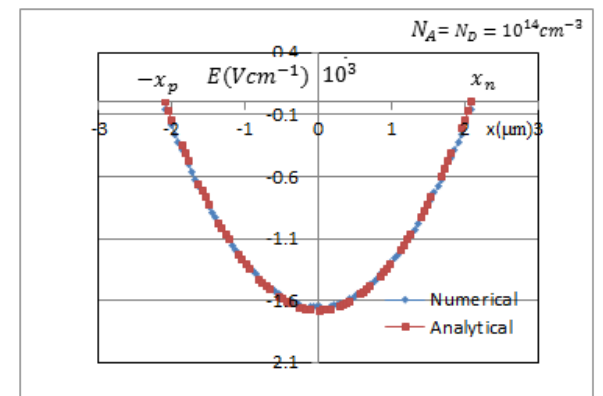


Fig. 6. Electric field for fixed charge density of impurities [N_A , N_D] within depletion layer

In the existence of free charges $p(x)$ and $n(x)$ in the depletion layer, the solution of Poisson's equation is difficult to solve analytically because free charges $p(x)$ and $n(x)$ follow exponential form as given by Eq. (2) and Eq. (3). Hence, a numerical method is implemented. Fig. 7 shows the free charge $p(x)$, $n(x)$ carriers appear as majority carriers (holes within the p-type material and electrons within n-type material) will partially neutralize the electrostatic charge arising from ionized impurity atoms. Using charge density $p(x)$, $n(x)$, and impurity concentrations in the numerical analysis we attend to charge distribution within the depletion layer as seen in Fig. 8. Close to the metallurgical junction, the charge density follows linearity on both sides, however, far away from the junction it deviated from linearity, due to the exponential form of free charge density. The high density of free charges will neutralize ionized impurity leading to reduce the width of the depletion layer in these regions.

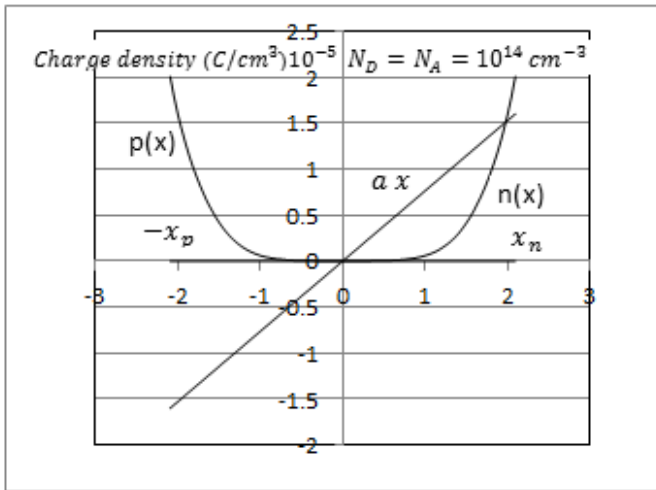


Fig. 7. Distribution of fixed $[N_A, N_D]$ and movable $[n(x), p(x)]$ charge density within depletion layer

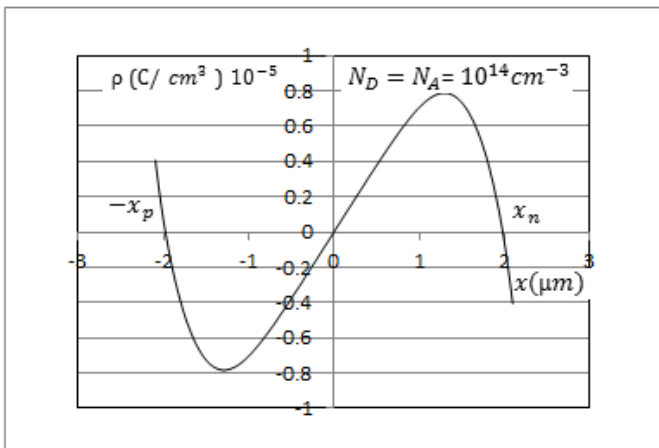


Fig. 8. Charge density ρ within depletion layer

Fig. 9 and Fig. 10 show the profile of the potential and electric field. The electric field is maximum at the metallurgical junction. The peaking of the electric field is because of the overall neutrality of the positive and negative charges in each side of the junction. The field lines will go from positive charges ends into negative charges. Thus, the highest number of electric field lines will be at the plane separating the two charge distributions, which is the metallurgical junction. Then, the electric field decreases with distance into both the p-type and n-type semiconductor. At the point $x=-1.98\mu\text{m}$ and $x=1.98\mu\text{m}$, the electric field changes its sign, and this is mainly due to no more ionized dopant exist beyond these points, hence, these points represented the boundary of depletion layers. The electric field and potential distributions within the depletion layer are significantly affected by free carriers.

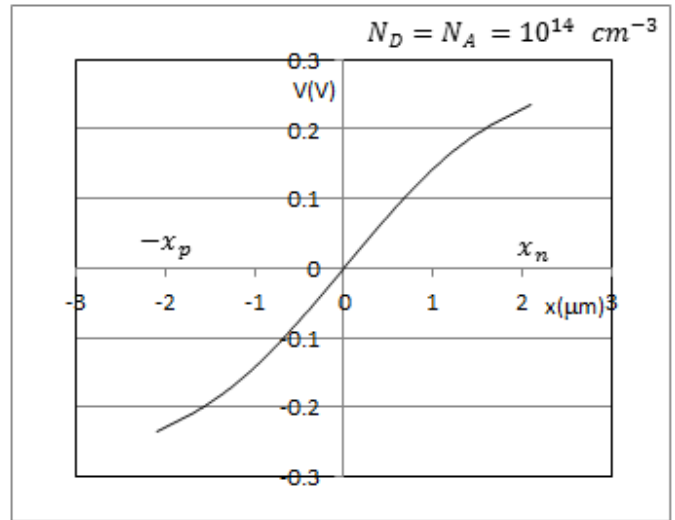


Fig. 9. The electrostatic potential within the depletion layer

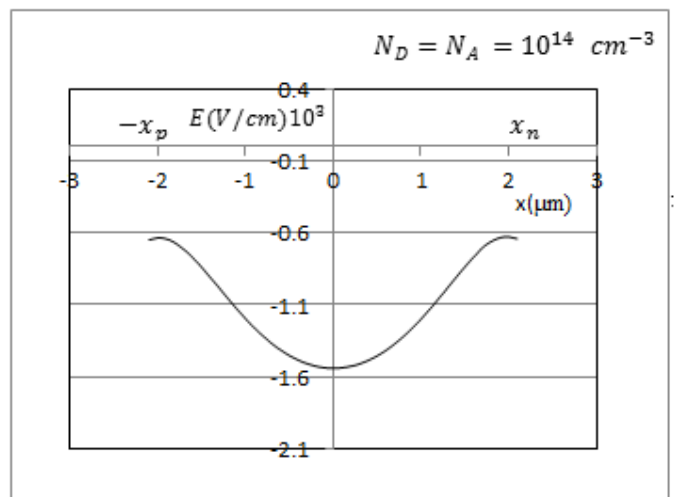


Fig. 10. The electric field within the depletion layer

As a matter of fact, the device is not in one dimension, our analysis extended into two dimensions (2D). To do the calculation in two dimensions, the charge density $\rho(x, y)$ has to be known. For simplicity in the calculation, the concentrations of charge along the y-axis were kept constant through each particular site y_i . Using this assumption, the profile of charge density is shown in Fig. 11. The potential and electric field of this charge distribution are given in Fig. 12 and Fig. 13.

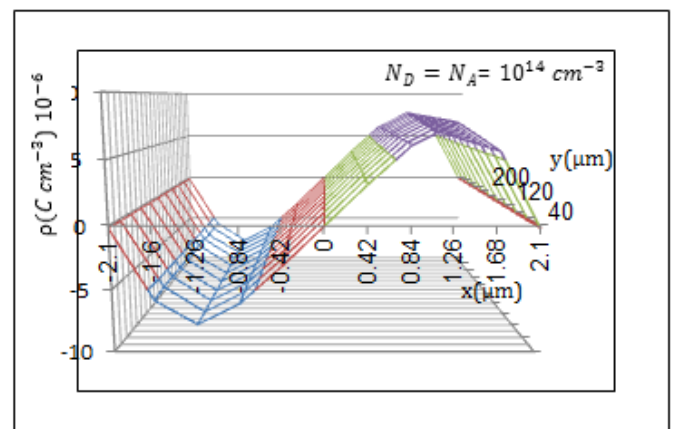


Fig. 11. The charge density ρ in [2D] within the depletion layer

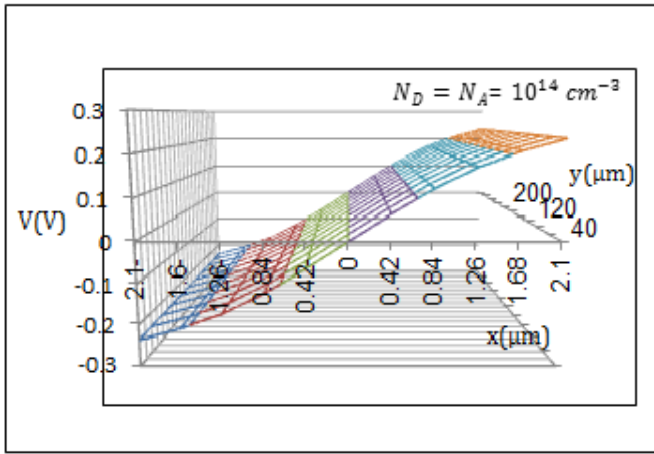


Fig. 12. The electrostatic potential in [2D] within the depletion layer

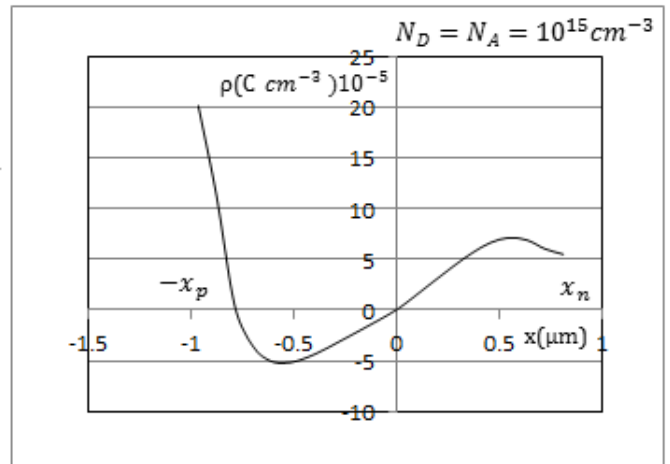


Fig. 15. Charge density ρ within depletion layer for doping rates $A=7 \times 10^{18} \text{ cm}^{-4}$ and $D=10^{19} \text{ cm}^{-4}$.

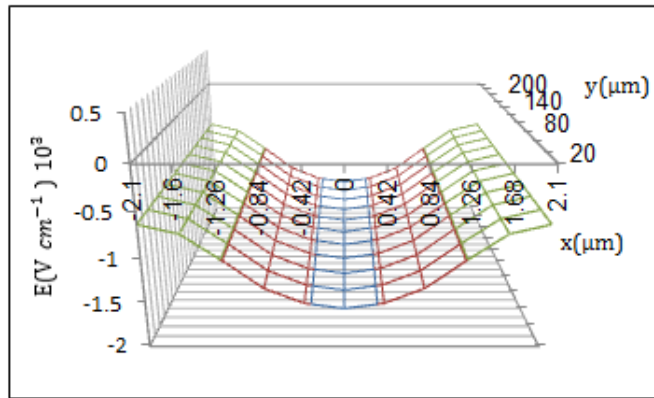


Fig. 13. The electric field in [2D] within the depletion layer

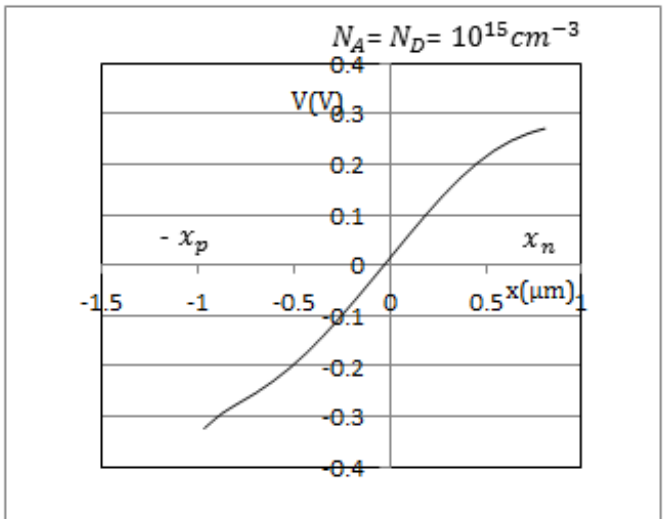


Fig. 16. The electrostatic potential within depletion layer for doping rates $A=7 \times 10^{18} \text{ cm}^{-4}$ and $D=10^{19} \text{ cm}^{-4}$.

A step of major importance in the theory of p-n junction is to get detailed information about the distribution of charge density within depletion layer, see Fig. 14. In the case of dopant concentration rates, $A=7 \times 10^{18} \text{ cm}^{-4}$ and $D=10^{19} \text{ cm}^{-4}$, the asymmetry distribution gives the resultant charge density as in Fig. 15. The depletion layer extends more in p-type material due to the high density of free charge $p(x)$ as seen in Fig. 14, which makes the neutralization of holes with impurity atoms more in this region of the junction. The boundary of the depletion layer reduces to $x=-0.78 \mu\text{m}$ instead of $x_p=-0.97 \mu\text{m}$. Fig. 16 and Fig. 17 show the potential and electric field in (1D). The electric field is maximum at the junction transition point and decreases with distance into both sides, but for p-type at $x=-0.78 \mu\text{m}$ for value $E=-2.23 \times 10^3 \text{ V/cm}$, the electric field changes its sign due to free charge $p(x)$ remaining in p-type as seen in Fig. 15.

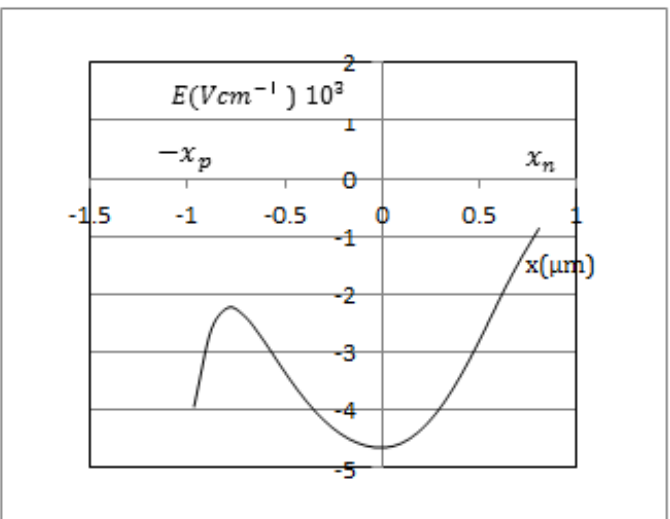


Fig. 17. The electric field within depletion layer for doping rates $A=7 \times 10^{18} \text{ cm}^{-4}$ and $D=10^{19} \text{ cm}^{-4}$.

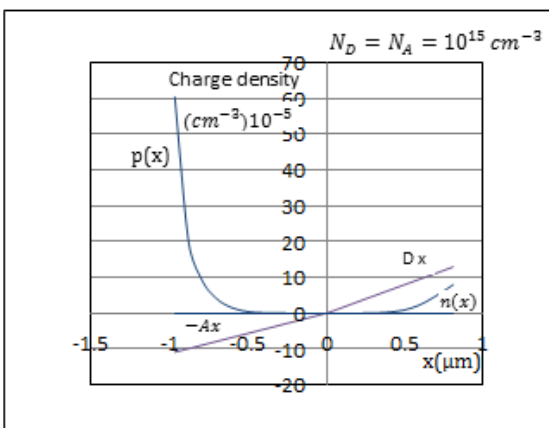


Fig. 14. Fixed $[Ax, Dx]$ and free $[p(x), n(x)]$ charge density within depletion layer for doping rates $A=7 \times 10^{18} \text{ cm}^{-4}$ and $D=10^{19} \text{ cm}^{-4}$.

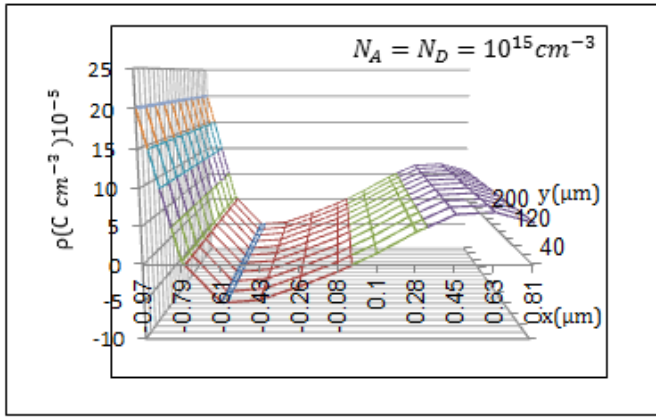


Fig. 18. Charge density ρ in [2D] within depletion layer for doping rates $A=7 \times 10^{18} \text{ cm}^{-4}$ and $D=10^{19} \text{ cm}^{-4}$.

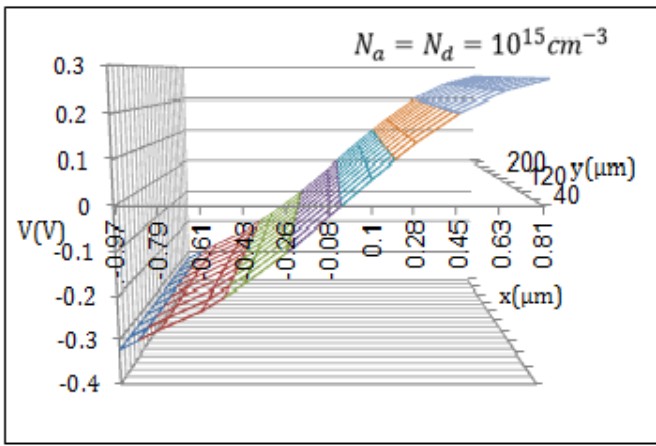


Fig. 19. Electrostatic potential in [2D] within depletion layer for doping rates $A=7 \times 10^{18} \text{ cm}^{-4}$ and $D=10^{19} \text{ cm}^{-4}$.

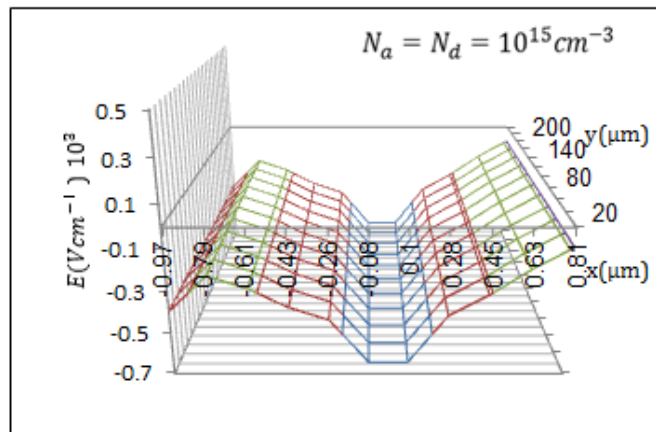


Fig. 20. The electric field in [2D] within depletion layer for doping rates $A=7 \times 10^{18} \text{ cm}^{-4}$ and $D=10^{19} \text{ cm}^{-4}$.

Fig. 18 shows the distribution of charge density in two dimensions (2D) for the case of asymmetry of dopant concentration rates (A, D). It is clear that asymmetry distribution yield a magnitude of depletion layer slightly greater in of low-doped region. Fig. 19 and Fig. 20 show the potential and electric field within the depletion layer for non-equal dopant concentration rates. Throughout the present calculation, the electric field is maximum at the junction, the depletion layer is assumed to be at locations where the electric field equals zero on each side of the junction or at points where the electric field changes its sign as explained in Fig. 15.

5. Conclusion

In this paper, we have attempted to provide a simple technique in the numerical analysis of semiconductor devices. The finite-difference method for the solution of Poisson's equation is discussed. First, the calculation was carried out for one-dimension (1D) using full charge density ρ (impurities $[N_A, N_D]$ and free charges $[n(x), p(x)]$). Then, calculations were extended into two-dimension (2D). The profile of charge density distribution; electric potential and electric field within the depletion layer were investigated. The effect of impurities in the depletion layer, electrostatic potential, and electric field was discussed. The method derived here is helpful to analyze non-linear impurities distribution such as exponential or hyper abrupt junction. The numerical solution of Poisson's equation in 2D can be combined with two equations of charge carriers (electrons, holes) to obtain the current density $J(x, y)$ of p-n junction solar cell in two dimensions.

Acknowledgment

We thank Dr. Khalaf J. Abed and Dr. Yousef O. Khazmi for their reviews, which substantially improved the manuscript. Their opinions are also greatly appreciated.

References

- Achoyan, A.Sh., Yesayan, A.E., Kazaryan, E.M., Petrosyn, S.G. (2002) 'Two-Dimensional p-n Junction under Equilibrium Conditions', *Semiconductors*, 36, 8, pp. 903–907
- Akinpelu, A., Akinojo, O.A., Usikalu, M.R., Onumejor, C.A. and Arijaje, T.E. (2018) A Numerical Simulation and Modeling of Poisson Equation for Solar Cell in 2 Dimensions. 2nd International Conference on Science and Sustainable Development. IOP Conf. Series: Earth and Environmental Science, 173, 012001
- Alexei, D. and Sajeev, J. (2012) 'Finite difference discretization of semiconductor drift-diffusion equations for nanowire solar cells', *Computer physics communication*, 183, pp. 2128-2135
- Benyam, M. and Purnachandra, R.K. (2015) 'Numerical Solution of a Two Dimensional Poisson Equation with Dirichlet Boundary Conditions', *American Journal of Applied Mathematics*, 3(6), pp. 297-304
- EL Faituri, F.Y.R. and Darkwi, A.Y. (2006) Computer simulation for current density in PN-silicon solar cells. Proceedings of the International Symposium on Solar Physics and Solar Eclipses (SPSE), Waw an Namus, pp. 163-171
- Green, M.A. (1982) *Solar cells, Operating Principles, Technology, and System Applications*. Prentice-Hall, Inc. Englewood Cliffs, N. J. pp 67
- Henry, B., Adnan, D., Dooie, T. and Seshadri, I. (1982) 'The forward biased, Abrupt p-n junction', *Solid-State Electronics*, 25, 2, pp. 105-113
- Kennedy, D.P., O'Brien, R.R. (1967) 'On the Mathematical Theory of the Linearly-Graded p-n Junction', *IBM Journal*, pp. 252-270
- Kosec, G. and Trobec, R. (2015) 'Simulation of semiconductor devices with a local numerical approach', *Engineering Analysis with Boundary Elements*, 50, pp. 69-75
- Newmen, M.A. (1997) *Semiconductor Physics and Devices, Basic Principles*, 2nd ed. IRWIN, pp 229-231
- Saeed, M. and Selvakumar, C.R. (1996) 'Calculation of Depletion Layer Thickness by Including the Mobile Carriers', *IEEE Transaction on Electron Devices*, 43, 1, pp. 185-188
- Shockley, W. (1949) 'The Theory of p-n junction in semiconductor and p-n junction Transistor', *B.S.T. J.*, pp. 435-439
- Sze, S.M. (1981) *Physics of Semiconductor Devices*, 2nd ed. John Wiley & Sons, Inc. pp. 74-84
- Zambuto, M. (1989) *Semiconductor Devices*, McGraw-Hill Book Company, Singapore, pp. 182-189.